

Properties of silver chloride and carbon screen printed patterns on different textiles

Textile Research Journal
2022, Vol. 92(15–16) 2711–2718
© The Author(s) 2021
Article reuse guidelines:
sagepub.com/journals-permissions
DOI: 10.1177/00405175211005039
journals.sagepub.com/home/trj



Victor Toral¹, Andreas Albrecht², Encarnación Castillo¹,
Antonio García¹ , Markus Becherer² and
Almudena Rivadeneyra¹ 

Abstract

Smart textiles, known also as e-textiles, are of great interest for the development of healthcare and wellness applications that require the embedding of electronic devices into the fabrics. Although many prototype proposals may be found in the literature, the generalization and commercialization of e-textiles is limited by the lack of cost-effective, standard fabrication processes that can be applied to a large variety of fabrics. In this contribution, we analyze the deposition of silver and carbon pastes by screen printing methods on a wide selection of daily-use textiles, to gain insight into the main features to be considered when developing cost-effective smart textiles. Results show the prospects offered by screen printing to create conductive patterns over textile and flexible materials with sheet resistances lower than $1 \Omega/\text{sq}$ and a good repeatability in the dimensions of the patterns.

Keywords

E-textiles, screen printing, silver chloride, carbon, sheet resistance

The boom of wearable electronics has driven the research on new materials applied to electronics, focusing on flexible and biocompatible electronic devices. As many wearable devices are meant to be integrated in the clothing of the user, or even the body, new electronic devices are required to adapt to this environment and to place the focus on user comfort. Contrary to traditional rigid electronics, flexible electronics offer great advantages in this situation.^{1,2}

These technologies can be applied to several real-life applications. One of the principal uses is the acquisition of biosignals, such as the electrocardiogram³ or the electromyogram, in this last case with applications for different kinds of prostheses.⁴ Examples of clothing for biosignal acquisition oriented to sport and health monitoring can be found in the literature.⁵ This is not limited to the academic field, and commercial products such as the socks developed by Sensoria^{®6} or the smart hat from 2XU⁷ are already available. E-textiles can be applied to other fields such as chemical analysis,

where applications for sweat analysis during physical activity⁸ have been presented.

Within this framework, conductive textiles allow us to create devices directly on the clothing of the user instead of attaching them to the fabric, thus improving integration and opening a wide range of new applications.^{9,10} Several methods for the development of these materials can be found in the literature through the fabrication of conductive fibers. These methods range from the use of novel 2D materials based on graphene, like carbon nanotubes or graphene derivatives, to the integration of conductive materials in the fibers of the textiles.^{11–13} Conductive polymers, such as

¹Department of Electronics and Computer Technology, University of Granada, Granada, Spain

²Institute for Nanoelectronics, Technical University of Munich, Germany

Corresponding author:

Almudena Rivadeneyra, University of Granada Campus Fuentenueva s/n Granada, 18071, Spain.

Email: arivadeneyra@ugr.es

poly(3,4-ethylenedioxythiophene) polystyrene sulfonate (PEDOT:PSS) have been also used to create this kind of fiber.^{14,15} While these methods can provide high levels of integration and conductivity, they are expensive and not efficient when large-area elements are needed. Printing techniques with conductive inks and pastes can be much more efficient, as they are able to overcome those drawbacks. Multiple techniques are available, such as screen, inkjet, gravure, or flexographic printing, or by coating the substrates.^{16,17} Spray deposition of conductive coatings can also be used for this purpose.¹⁸ However, screen printing is the technique that best adapts to different textile substrates. Furthermore, it requires fewer complex systems than gravure, flexographic, or inkjet printing. Compared with spray coating, the availability of inks is also higher for screen printing. For these reasons this technique is widely used to create conductive patterns on textiles.^{19–21} It has been used in the creation of wearable antennas and transmission lines,^{22,23} or wearable flexible electrodes.^{24–26}

With all the above in mind, the use of screen printing with a wide range of fabric substrates is studied in this contribution, using carbon and silver pastes to print the patterns. This study first covers the physical characteristics of the patterns, such as thickness and conductivity, with different pastes. After that, the influence of the substrate on conductivity is studied in different substrates, from latex gloves to sanitary napkins, using silver chloride printed patterns for the measurements.

Materials and methods

As detailed above, screen printing was selected for this study due to its versatility to print on different substrates. A manual screen printer from Siebdruck Versand was used to deposit the pastes.²⁷ To print the conductive sections, the silver chloride paste EDAG 6038E SS E&C from Loctite²⁸ and the carbon paste C220 from Applied Ink Solutions²⁹ were selected. Three different screens were used, depending on the viscosity of the paste. To achieve the maximum printing accuracy, the highest possible number of threads per centimeter, or mesh, is needed. However, this

type of screen is not suitable for high-viscosity pastes. For this reason, a 120 T/cm screen was used with the silver chloride paste, whereas a 47 T/cm screen was used for the carbon paste. Dielectric sections were also printed using the 47 T/cm screen and the TD-642 dielectric paste from Applied Ink Solutions. Furthermore, the silver paste CI-1036 from Engineered Conductive Materials, LLC with an 80 T/cm screen was used for simpler lines.³⁰ These pastes were selected in order to cover a wide range of applications, and they were used without any modification in their formulation. As they are biocompatible, they are widely used in the fabrication of electrodes for bio-signal acquisition. The application of these materials directly on textiles could enable their use for long-term monitoring.³¹

In this study different types of substrates were also considered. The selection was done aiming to cover a wide range of stretchable materials, flexible materials, and non-stretchable porous materials, all of them usually present in industry or daily life, including some non-textiles. The chosen materials are shown in Table 1. This selection was intended to show a realistic representation of the applicability of smart textiles and the conversion of regular textiles into smart textiles. The layer arrangement shown in Figure 1 was printed over these substrates, including the conductive wiring with a dielectric covering on top.

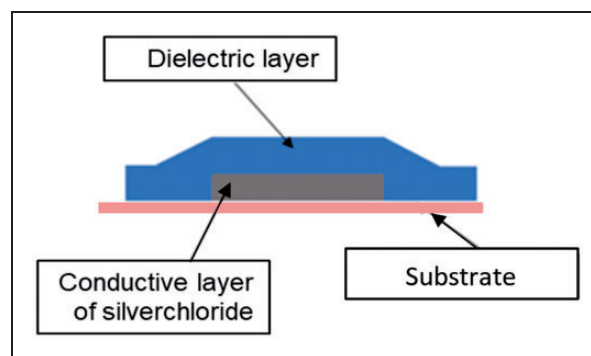


Figure 1. Cross-section scheme of the printed layers using the example of the printing of a conductor made of silver chloride with an overlying insulator.

Table 1. Selected materials (non-textiles marked with *)

Stretchable	Flexible	Non-stretchable
Bandage	Dishcloth (cross-linked cellulose and cotton)	Bandage interior
Rubber glove*	Kleenex*	Diaper
Latex glove*		PET*
Acrylic wool glove		Sanitary napkin
Nylon tights		

Two aspects were analyzed to study the created patterns: first, the profile of a printed line, focusing on the height, the roughness, and the reproducibility of the pattern, and, additionally, the ohmic resistance of the patterns printed over different substrates. For the profile measurements, a Dektak XT surface profilometer from Bruker was used, while microscope images of the printed structures were acquired with a DinoLite AM4115ZT microscope. For the roughness, the surface parameter R_a of the printed line was analyzed. This parameter is defined as:

$$R_a = \frac{1}{l} \int_0^l |z(x)| dx$$

where l is the length of the analyzed profile and $z(x)$ is the deviation from the average height of the measured profile.

On the other hand, the sheet resistance was also analyzed on the different substrates. This measurement was carried out using a four-point probe head from Jandel connected to a B2901A Keysight source measuring unit. A constant current of 10 μA was sourced for all measurements. The sheet resistance can then be measured following the same method described by Valdes.³² As the roughness of the substrate can affect the sheet resistance and in order to have a reference, the same patterns were printed over polyethylene terephthalate (PET) films, where roughness is much lower than on the rest of substrates. Thus, on PET, the carbon paste exhibited a sheet resistance of 15 $\Omega/\text{sq.}$, while the silver chloride's was 0.05 $\Omega/\text{sq.}$

For stretchable materials, bending tests were carried out in addition to static tests. The bending tests were done with a custom-made setup as described by Albretch et al.³³ This bending test was thus started with small strains of 0.1%, which were gradually increased until the breaking point. For the materials enduring more strain, the sheet resistance was measured after 10 consecutive bending cycles with strains below the breaking point, to study how the mechanical efforts in the substrate impacted the sheet resistance.

Results and discussion

Profile characteristics

The first study investigated the profile characteristics of the printed lines. To avoid any influence in this regard from the properties of the different substrates, several sets of lines, as described below, were printed on the reference PET substrate. It must be also noted that the solid content of the silver chloride paste, according to the manufacturer's data sheet,²⁸ is 66%, with a 9:1

ratio of silver and silver chloride, and a mixture of diethylene glycol monobutyl ether and methoxypropyl acetate as solvents. In the case of the carbon paste, the solid content of graphite is 42%, with gamma-butyrolactone and dimethyl glutarate as solvents.²⁹

Figure 2 shows the thickness comparison between a printed line of carbon paste and one printed with the silver chloride paste. Black lines represent the average thickness of these lines. In the case of the carbon paste, this average refers to the thickness measured between 0.02 mm and 1.38 mm in the Distance axis of Figure 2, while for silver chloride the average thickness covers measurements from 0.054 mm to 1.33 mm in the Distance axis of Figure 2. The thickness measured in the carbon line was 5.18 μm , whereas the silver chloride line thickness was 6.73 μm . The silver chloride paste line was thus approximately 30% thicker than the carbon paste one, which is mostly due to the lower solid content of the carbon paste.

The roughness of the patterns was compared with the R_a values of each profile. Thus, carbon ink printed lines showed an R_a value of 1.19 μm , while for the silver chloride it was 0.93 μm . Carbon lines were thus 22% rougher than silver paste ones and, taking into account that the carbon lines were thinner, this results in a much irregular surface.

Comparing the line widths, silver chloride lines were 1.24 mm wide, whereas for carbon this width was 1.36 mm. Both differ from the 1 mm width of the mask by approximately 0.3 mm, because the paste is pushed slightly beyond the edges of the mask.

To compare the reproducibility of the lines, a pattern with several adjacent lines was printed. In Figure 3, the profiles measured with both carbon and silver pastes are shown. The average line height was calculated discarding the gaps between the lines, thus calculating the individual thickness of the lines and averaging all of them. The mean height of silver lines was 6.86 μm with a standard deviation of 0.44 μm , and for carbon lines the mean was 5.42 μm with a standard deviation of 0.67 μm . From these values, it may be noticed that the individual lines of both printed structures presented uniform thickness. However, the silver lines showed higher thickness than the carbon ones, being 1.44 μm thicker, which is consistent with the results obtained above for single lines. The variability of the lines was under 12% in both cases, although the carbon lines were more variable than the silver chloride lines, as expected from the roughness results. Regarding the width of the lines, the carbon lines were 1.40 mm wide on average with standard deviation of 38 μm , and the silver chloride lines were 1.24 mm wide with standard deviation of 34 μm . The variation in both cases was 2.7% of the mean value.

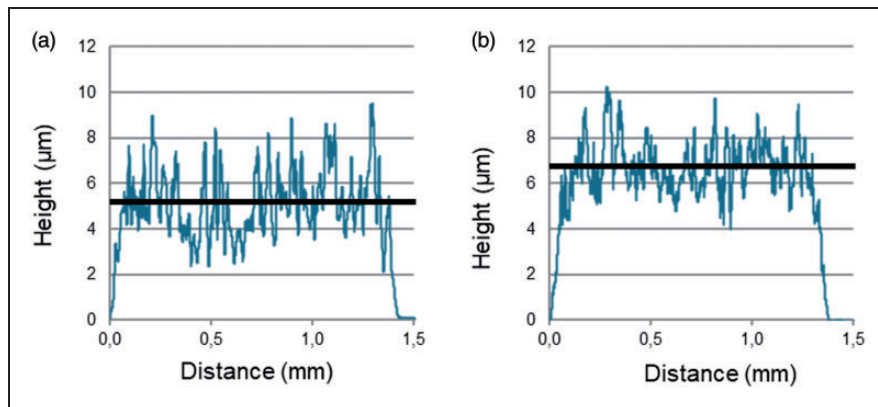


Figure 2. Comparison of the profile diagram of a printed line: (a) carbon, (b) silver chloride (profilometer measurements in blue, mean values in black).

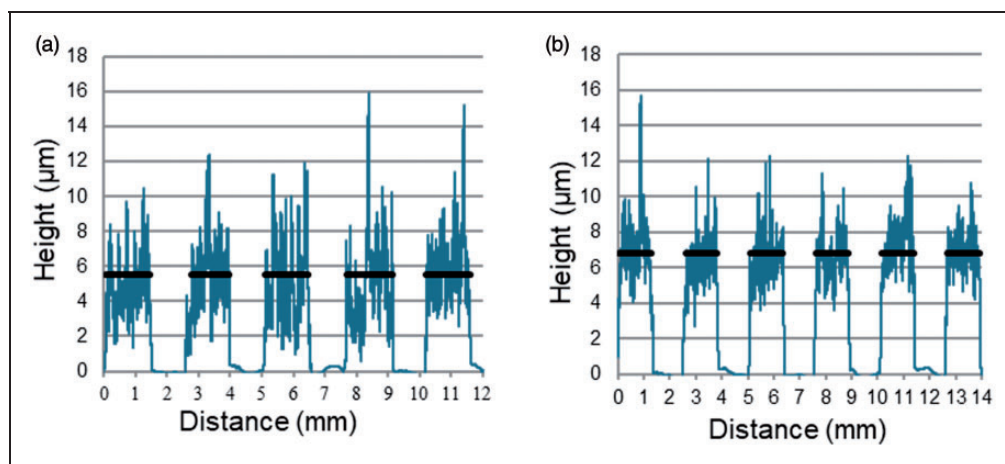


Figure 3. Comparison of the profile diagrams of several printed lines: (a) carbon, (b) silver chloride (profilometer measurements in blue, mean values in black).

To create multilayer structures, dielectric layers are required between consecutive conductive layers in order to avoid short circuits. Thus, the profile of a dielectric layer printed over a line of silver chloride, as shown in Figure 4(a), was also studied. In this type of structure, as the dielectric layer is the base for the next conductive layer, the roughness of the printed dielectric is key. A possible solution to reduce the roughness of the dielectric is to print several layers of dielectric over the silver chloride line. Figure 4(b) shows the profile of such a structure. The average thickness was studied in those zones that did not have silver chloride under the dielectric. The results showed a thickness of 4.85 µm for a single layer and 11.52 µm for the multiple-layer print.

The standard deviation of the measured values was 0.56 µm for a single layer and 1.95 µm for four layers. The surface of the single layer was quite smooth with a

R_a value of 0.43 µm, while the four-layer structure showed some roughness, with R_a of 1.42 µm, which can be explained by the highest thickness measured between 0.5 mm and 2.5 mm (in the Distance axis of Figure 4(b)) and probably due to a lower pressure in this zone during printing. Two elevations at the printing edges are noticeable, as there is always more paste at the end of the screen, i.e. at the transition from the permeable to the impermeable part of the sieve, than in the middle part of the screen. As this multilayer structure was printed several times and the squeegee was thus drawn from right to left and left to right over the screen, the increase found on both sides is higher.

The results of the bending test showed noticeable differences between materials. The maximum possible strain, i.e. the strain at the breaking point, for the bandage was below 2%, whereas the maximum strain for the acrylic wool glove and the nylon tights was up to

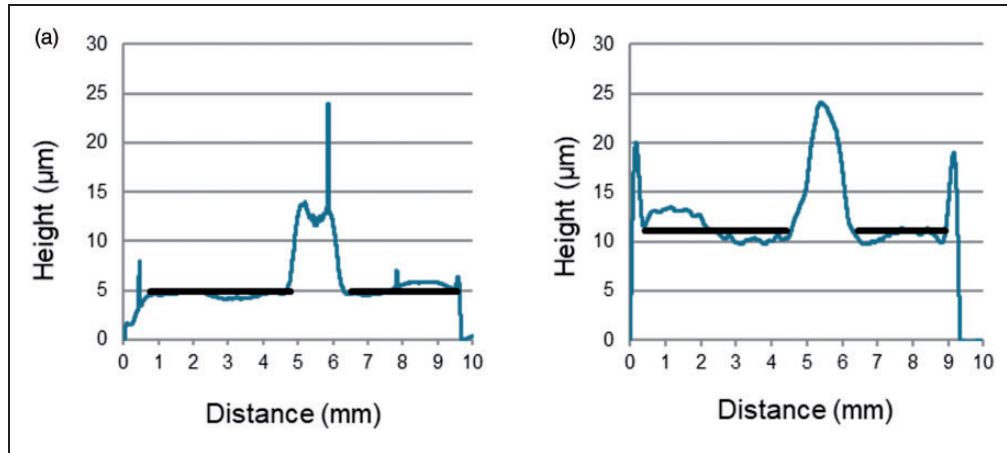


Figure 4. Comparison of the profile diagrams of a printed silver chloride line with: (a) single-layer printed dielectric, (b) multiple-layer printed dielectric (profilometer measurement in blue, mean in black).

12%. The rubber and latex substrates could bear even higher strains, up to 32% and 35%, respectively.

Finally, preliminary manual rubbing tests were carried out over the PET substrate with both pastes, carbon and silver chloride. The different printings were rubbed for 70 cycles using a microfiber cloth, and the ohmic resistance was measured after every 10 cycles. With this, results showed two differentiated behaviors: the silver chloride paste did not change its resistance after 70 cycles, whereas the carbon paste increased its resistance by around a 20% after 70 cycles. Even with wear beginning to be visually appreciable in both pastes, only the carbon paste's resistance was altered.

Substrate influence on ohmic resistance

After the study above on the reference PET substrate, silver chloride conductive lines were printed on the different substrates in order to measure printed sheet resistances. As the silver chloride paste resulted in smoother, more conductive and more durable patterns, only silver chloride was considered on the different substrates in Table 1 for this evaluation of the influence of the substrate on the ohmic resistance. Microscope images of the most representative substrates are shown in Figure 5. These enable a closer examination of the surface structures of the substrates, as well as of the printed structures, in order to draw possible conclusions regarding the respective conductivity of the printing. The same magnification was chosen for all substrates. The rubber glove (Figure 5(a)) presents a very smooth surface compared with the other substrates, as well as the layer printed on it. This means that there are no irregularities, in the form of holes or the like, recognizable in the layer. It is thus possible to

print a precise edge on this material. Apparently, there are no indications of a reduced conductivity. The images of the sanitary napkin (Figure 5(b)), the acrylic wool glove (Figure 5(c)) and the nylon tights (Figure 5(d)) reveal a thread-like structure, with a significantly coarser fabric in the sanitary napkin and the acrylic wool glove. These substrates are characterized by the multi-layered nature of the material, i.e. the fact that several fibers lie on top of and underneath each other, which is confirmed by the partially blurred microscope images.

The dishcloth textile (Figure 5(e)) is characterized by a coarse-pored structure, so larger air gaps can be observed and the surface is therefore uneven. The printed layer, on the other hand, presents little unevenness and few holes or other defects.

Table 2 lists all the measured sheet resistances of the printed silver on the respective materials. The results show that all printed structures were conductive but presented different sheet resistances. Apart from the values measured for the nylon tights, all values are under $1 \Omega/\text{sq}$. It is striking that the printed silver paste conducts best on the dishcloth, even better than on the PET reference. This can be attributed to the fact that the substrate material itself is slightly conductive, as a resistance in the mega-ohm range can be measured for this material without any deposited conductive layer. In addition, the holes visible in Figure 5(e) are filled with conductive paste and the sponge-like tissue is able to absorb paste, thus resulting in many contact points between the silver layers even deeper in the tissue. Thin fabrics with a fine structure like the bandage and the Kleenex also show low sheet resistances when compared with the rest of the tested substrates. These are comparable to the values on PET. Although less paste can be absorbed here, the relatively smooth

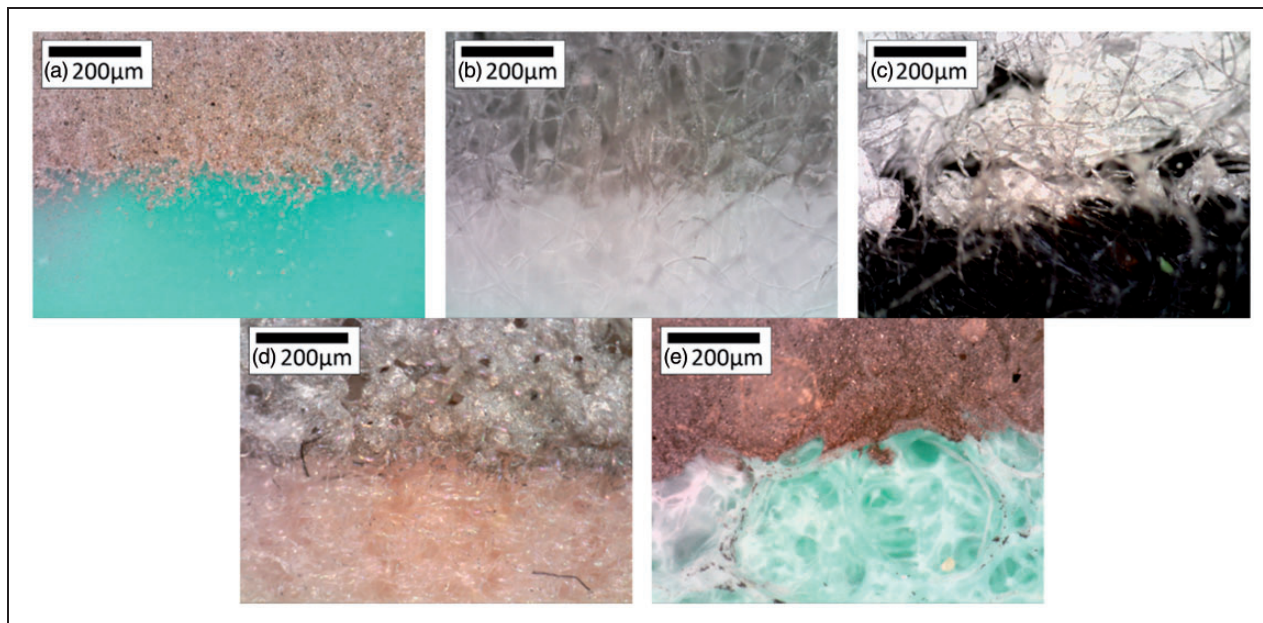


Figure 5. Selected microscope images of different substrates with printed silver paste: (a) rubber glove; (b) sanitary napkin; (c) fabric glove; (d) nylon tights; (e) dishcloth. The printed silver can be observed in the top half of the images, the unprinted substrate in the bottom areas.

Table 2. Sheet resistance of printed silver on different materials. Errors are calculated as the standard deviation of five different samples

Material	R (mΩ/sq)
Dishcloth	100 ± 50
Bandage	320 ± 80
Kleenex	380 ± 70
Bandage interior	430 ± 50
Diaper	540 ± 50
PET	586 ± 5
Sanitary napkin	630 ± 60
Rubber glove	660 ± 30
Latex glove	790 ± 30
Acrylic wool glove	940 ± 10
Nylon tights	5000 ± 200

surfaces are a good prerequisite for a layer with few holes, which reduces the resistance. In any case, as illustrated by the standard deviations of the measurements in Table 2, measurement dispersion is observed for all the materials when compared with PET, which is an especially smooth substrate and ideal for printing applications. These deviations could thus be reduced by flattening the substrates with a preprint of a dielectric layer.

Coarser materials, such as the diaper, the sanitary napkin, or the acrylic wool glove, generate more and larger holes (Figure 5(b) and Figure 5(c)), which could be related to a higher sheet resistance. However, this is

not observed in all cases. For example, although the fibers in the nylon tights are thinner than in the fabrics just mentioned (see Figure 5(d)), the sheet resistance is higher in this case. As more paste can penetrate deeper into some of the fibrous materials that are more absorbent due to their purpose, such as the dishcloth and the bandage, and, although the structure reveals holes from above, they can still provide enough contact points. The rubber and latex gloves also confirm the effect of a smooth surface, as they show a comparatively high sheet resistance.

Bending tests showed low influence of the mechanical effort on the sheet resistance. For the latex gloves, the variation in the sheet resistance was 10% and the change in sheet resistance for the rubber ones was 8%. This small difference is probably due to the lower stretchability of rubber gloves. Finally, although no deep study on the useful life of the patterns was carried out, some surface oxidation was observed in some patterns that were not encapsulated with dielectric. Thus, a dielectric coating should avoid this effect.

Conclusions

Screen printing with conductive pastes over different flexible and stretchable substrates was studied in this work. First, thickness, roughness, and width of the printed patterns were analyzed. The results show uniform and highly reproducible patterns for both of the used pastes. In terms of thickness and width of the

patterns, printed variability was less than 12% in thickness and less than 2.7% in width. Regarding the roughness of the patterns, it was under 1.19 μm , with carbon patterns the roughest. This all demonstrates how the printings can be easily replicated with consistent repeatability. Also, the capability to create multilayer structures was illustrated through the use of the dielectric paste TD-642 between conductive layers. The best option to create this multilayer structure was to only print a dielectric layer, as it resulted in a 30% smoother surface.

In addition, the sheet resistance of the patterns was studied over several textile materials using the silver chloride paste, as it provided the most uniform patterns. For all of the materials but for nylon, the resistances were under 1 Ω/sq . The materials with lower resistance were those able to absorb the paste, thus creating a conductive surface that penetrates the material. Materials with coarser fibrous substrates, such as the acrylic wool gloves, were those with lower performance, as the paste over those materials created a surface with many defects and uneven surfaces.

With all of the above, we have demonstrated the capability of screen printing to easily create conductive flexible patterns over textile and flexible materials with sheet resistances lower than 1 Ω/sq and with a good repeatability of the patterns, even when created with multiple layers of dielectric. With these results, the possibilities of creating circuits on textile and flexible materials have been illustrated, thus opening a wide range of applications. Direct applications may include the acquisition of biosignals through electrodes printed on the clothing, or the use of textiles for interconnection with other developed patches, which can create a complete body sensor network in the user clothing. Furthermore, the combination of these conductive patterns with sensitive substances could allow the development of wearable sensors for chemical substances, biomechanical analysis, or environmental variable sensing.

Declaration of conflicting interests

The author(s) declared no potential conflicts of interest with respect to the research, authorship, and/or publication of this article.

Funding

The author(s) disclosed receipt of the following financial support for the research, authorship, and/or publication of this article: This work has been supported by the BBVA Foundation through a 2019 Leonardo Grant for Researchers and Cultural Creators; and by the Spanish Ministry of Education, Culture and Sport through the doctoral grant FPU18/01376.

ORCID iDs

Antonio García  <https://orcid.org/0000-0003-3533-4660>
 Almudena Rivadeneyra  <https://orcid.org/0000-0001-8133-1992>

References

- Nathan A, Ahnood A, Cole MT, et al. Flexible electronics: The next ubiquitous platform. *Proc IEEE* 2012; 100: 1486–1517.
- Axisa F, Schmitt PM, Gehin C, et al. Flexible technologies and smart clothing for citizen medicine, home healthcare, and disease prevention. *IEEE Trans Inf Technol Biomed* 2005; 9: 325–336.
- Wu W, Pirbhulal S, Sangaiah AK, et al. Optimization of signal quality over comfortability of textile electrodes for ECG monitoring in fog computing based medical applications. *Futur Gener Comput Syst* 2018; 86: 515–526.
- Secco EL, Moutschen C, Maereg AT, et al. Development of a Sustainable and Ergonomic Interface for the EMG Control of Prosthetic Hands. In: *International Conference on Wireless Mobile Communication and Healthcare*, 2016, pp. 321–327. Springer, Cham.
- Paradiso R, De Toma G, Mancuso C. Smart Textile Suit. In: Tamura T and Chen W (eds) *Seamless Healthcare Monitoring*. 2018, pp.251–277. Cham: Springer International Publishing.
- Sensoria Fitness, <https://store.sensoriafitness.com/one-additional-pair-of-smart-sock-v2-0/> (accessed 20 December 2020).
- 2XU, https://www.2xu.com/us/p/tracking-hat/UQ4194f.html?lang=en_US (accessed 20 December 2020).
- Coyle S, Lau K-T, Moyna N, et al. BIOTEX—biosensing textiles for personalised healthcare management. *IEEE Trans Inf Technol Biomed* 2010; 14: 364–370.
- (Kelvin) Fu K, Padbury R, Toprakci O, et al. Conductive textiles. In: *Engineering of High-Performance Textiles*. Elsevier, pp.305–334.
- Wu R, Ma L, Patil A, et al. All-textile electronic skin enabled by highly elastic spacer fabric and conductive fibers. *ACS Appl Mater Interfaces* 2019; 11: 33336–33346.
- Neves AIS, Rodrigues DP, De Sanctis A, et al. Towards conductive textiles: Coating polymeric fibres with graphene. *Sci Rep* 2017; 7: 1–10.
- Xue CH, Chen J, Yin W, et al. Superhydrophobic conductive textiles with antibacterial property by coating fibers with silver nanoparticles. *Appl Surf Sci* 2012; 258: 2468–2472.
- Zhao Y, Wang J, Li Z, et al. Washable, durable and flame retardant conductive textiles based on reduced graphene oxide modification. *Cellulose* 2020; 27: 1763–1771.
- Kuhn HH, Kimbrell WC, Fowler JE, et al. Properties and applications of conductive textiles. *Synth Met* 1993; 57: 3707–3712.
- Knittel D and Schollmeyer E. Electrically high-conductive textiles. *Synth Met* 2009; 159: 1433–1437.
- Khan S, Lorenzelli L, Dahiya RS. Technologies for printing sensors and electronics over large flexible substrates: A review. *IEEE Sens J* 2015; 15: 3164–3185.

17. Maheshwari N, Abd-Ellah M and Goldthorpe IA. Transfer printing of silver nanowire conductive ink for e-textile applications. *Flex Print Electron* 2019; 4: 025005.
18. Samanta A and Bordes R. Conductive textiles prepared by spray coating of water-based graphene dispersions. *RSC Adv* 2020; 10: 2396–2403.
19. Hobby A. Fundamentals of screens for electronics screen printing. *Circuit World* 1990; 16: 16–28.
20. Nisato G, Lupo D and Ganz S. *Organic and printed electronics: Fundamentals and applications*. Singapore: CRC Press, Pan Stanford Publishing, 2016.
21. Kazani I, Hertleer C, De Mey G, et al. Electrical conductive textiles obtained by screen printing. *Fibres Text East Eur* 2012; 1(90): 57–63.
22. Locher I and Tröster G. Screen-printed textile transmission lines. *Text Res J* 2007; 77: 837–842.
23. Scarpello ML, Kazani I, Hertleer C, et al. Stability and efficiency of screen-printed wearable and washable antennas. *IEEE Antennas Wirel Propag Lett* 2012; 11: 838–841.
24. Paul G, Torah R, Beeby S, et al. The development of screen printed conductive networks on textiles for biopotential monitoring applications. *Sensors Actuators A Phys* 2014; 206: 35–41.
25. Yang K, Freeman C, Torah R, et al. Screen printed fabric electrode array for wearable functional electrical stimulation. *Sensors Actuators A Phys* 2014; 213: 108–115.
26. Yang K, Torah R, Wei Y, et al. Waterproof and durable screen printed silver conductive tracks on textiles. *Text Res J* 2013; 83: 2023–2031.
27. Siebdruck Versand. Siebdruck-versand webpage, <https://www.siebdruck-versand.de/> (accessed 19 May 2020).
28. Safety Datasheet EDAG 6038E, [https://mysds.henkel.com/SAP_GATEWAY/odata/SAP/YPSSWH_DOO_SRV//DocContentSet\(Appid='YPSSW_SDSUA',Matnr='000000000001837601',Matnrcomp='',Subid='000000487422',Subidcomp='',Sbgvid='MSDS_UT_US',Laiso='EN'\)/DocContentData/\\$value](https://mysds.henkel.com/SAP_GATEWAY/odata/SAP/YPSSWH_DOO_SRV//DocContentSet(Appid='YPSSW_SDSUA',Matnr='000000000001837601',Matnrcomp='',Subid='000000487422',Subidcomp='',Sbgvid='MSDS_UT_US',Laiso='EN')/DocContentData/$value) (accessed 21 October 2020).
29. C-220 Safety Data Sheet, <https://kayakuam.com/wp-content/uploads/2020/03/SDS-C-220-Carbon-Resistive-Ink-US.pdf> (accessed 21 October 2020).
30. CI-1036 Technical Data Sheet, <http://www.conductives.com/pdfs/CI-1036.pdf> (accessed 21 October 2020).
31. Ankhili A, Tao X, Cochrane C, et al. Comparative study on conductive knitted fabric electrodes for long-term electrocardiography monitoring: Silver-plated and PEDOT:PSS coated fabrics. *Sensors* 2018; 18: 3890.
32. Valdes L. Resistivity measurements on germanium for transistors. *Proc IRE* 1954; 42: 420–427.
33. Albrecht A, Bobinger M, Salmerón J, et al. Over-stretching tolerant conductors on rubber films by inkjet-printing silver nanoparticles for wearables. *Polymers (Basel)* 2018; 10: 1413.